*J Forensic Sci,* January 2009, Vol. 54, No. 1
doi: 10.1111/j.1556-4029.2008.00930.x
Available online at: www.blackwell-synergy.com

*Tsadok Tsach,*[1] *M.Sc.; Eliezer Landau,*[1] *M.Sc.; Yaron Shor,*[1] *M.Sc.; Nikolai Volkov,*[1] *M.D.; and Alan Chaikovsky,*[2] *B.Sc.*

# Estimating Projectile Perpendicular Impact Velocity on Metal Sheet Targets from the Shape of the Target Hole

**ABSTRACT:** The correlation between bullet hole shapes in metal and projectile impact velocity was examined. A series of shots were fired from an M-16A1 assault rifle of 5.56 mm caliber toward a 1-mm thick metal target. All shots were fired at a perpendicular angle to the metal sheets, and the velocity was measured just before the projectile hit the target. Velocities ranged between 400 and 900 m/sec. From the replica of the shooting hole, a perpendicular plane was created, showing the symmetrical properties of the hole. The best mathematical equation describing the shape of the entrance hole was the exponential function in the form:

$$Y_x = A + B\mathrm{e}^{kx}$$

The empirical equation of the hole defined using the regression method is:

$$Y_{x,V} = \frac{8.268}{V^{0.578018}}\mathrm{e}^{\left(\frac{0.584x}{V^{0.005}}\right)}$$

This equation describes the general shape of shooting holes created by velocities ranging from 440 to 750 m/sec. From this equation, one can estimate the bullet velocity when it hits the target.

**KEYWORDS:** forensic science, Levenberg-Marquardt, projectile penetration, shooting distance estimation, projectile hole shape

There has been an increase in shooting incidents in Israel during recent years. Police investigation of these incidents often requires determination of the shooter's position. The shooting direction is generally established by observing the bullet holes, but it is usually difficult to determine the shooting distance.

Projectile penetration is affected by shooting distance and is influenced by weapon type, projectile shape, velocity, and ballistic properties. Projectile penetration of a metal target has previously been investigated (1,2). The primary goals of these works were: (i) to improve the penetration of the projectile through metal and (ii) to improve target resistance to projectile penetration. There has been no forensic examination of projectile penetration to determine shooting distance.

Internal stress and strain develop during the interaction between a projectile and metal target, due to the momentum (3) caused from the projectile colliding with the target. The stress created inside the metal is comprised of both compression and shearing (2). Stress created from a high velocity projectile is greater than the maximum plastic stress (ultimate tensile strengths) of the metal. Metal will behave as if it were brittle, when pierced by the projectile, due to the intense impact force.

Numerous parameters can influence the projectile flight to the target (4), e.g., the type of weapon fired and its barrel diameter, and the projectile's shape, velocity, and ballistic properties. These parameters influence the kinetic energy ($E_k$) of the projectile during its flight until it reaches the target. To estimate the striking velocity of a projectile, it is necessary to know the kinetic energy of the projectile and the subsequent deformation of the target.

The equation of kinetic energy that describes the projectile flight is

$$E_k = \frac{mV^2}{2}\text{joules} \quad (1)$$

where $m$ is the mass of the projectile and $V$ is the velocity of the projectile.

Part of the energy produces projectile deformation, part is transferred to the target by plastic deformation, and a small fraction is converted to heat transfer. The remaining energy continues with the projectile after it leaves the target.

The penetration force is related to the metal properties of the target and the kinetic energy of the projectile. As the square of the velocity has the greatest influence on the kinetic energy, the equation that describes the deformation rate (5) is

$$\frac{\partial\varepsilon}{\partial t} = f(\sigma,\ \varepsilon,\ T,\ S) \quad (2)$$

where $t$ is the time, $\sigma$ is the stress, $\varepsilon$ is deformation, $T$ is the temperature, and $S$ is the metal properties.

There are several methods to estimate shooting distance of a projectile from a weapon to a target and are as follows:

[1]Toolmarks and Materials Laboratory, DIFS, Israel Police Headquarters, Jerusalem 91906, Israel.
[2]Photography Laboratory, DIFS, Israel Police Headquarters, Jerusalem 91906, Israel.

Received 16 Dec. 2007; and in revised form 26 Apr. 2008; accepted 28 Apr. 2008.

- Measuring the time between firing and impact of the target using microphone and soundcard (6). This method is mainly applicable under laboratory condition in shootings from long distances.
- Identification of nitrite residue from ammunition powder found near or on the edge of the hole (7–9). This method is effective in short range firing (only a few meters).
- Finding the antimony concentration on the target resulting from the primer residues (10). This method is effective up to 3 m.
- Gun shot residue identification on the target (11,12).
- Estimating the distance by projectile deformation (13–16). This method can estimate distances between 200 and 400 m.

The goal of this research was to provide an objective procedure for using the contours of the entrance hole on the target to estimate the projectile velocity, based solely on a mathematical equation.

## Materials and Methods

Several series of shots were fired at a tin target 20 × 20 cm and 1 mm thick; the weapon used was a short M-16A1 assault rifle caliber 5.56 × 45 mm (COLT Ltd., Hartford, CT). Velocity was measured just before impact, using a chronograph model 83 manufactured by Oehler (Austin, TX). The measured velocity ranged between 400 and 900 m/sec. Each series consisted of four to five shots fired on a police-firing range. Velocities were lowered by reducing the powder charge (17). This reduction in velocity was used to simulate longer shooting distances as calculated using a ballistic program (18), after obtaining the velocity of the projectiles (see Table 1). The velocity reduction was done to make sure that the projectiles hit the target perpendicularly.

Silicon casts of the shooting holes were created to preserve the holes' shape. The silicon duplicate was photographed perpendicular to the projectile's entrance. Coordination of the geometric shape contour of the hole was registered by Adobe Photoshop® software (version 7.0).

The software that converts the coordination of the hole's shape to the equation uses the statistic numeric procedure (Levenberg-Marquardt, "Mathematica for Students," Wolfram Research, Inc., Champaign, IL, 1997). This method gradually shifts the search of the function parameters for the minimum iteration of a given function, from steepest descent to quadratic minimization. The statistic numeric procedure is a combination of two numeric procedures that helps obtain an optimal function with minimal iteration. The first procedure, steepest-descent uses the initial parameters (B, k, $\alpha$, $\beta$) when they may have a large deviation from the optimal solution that describes the curve. This yields the second procedure (quadratic minimization), which quickly leads to the optimal solution.

TABLE 1—*Correlation between ammunition powder weight to the velocity and the shooting distance for caliber 5.56 × 45 mm (the two right columns).*

| Muzzle Velocity (m/sec) | Ammunition Powder Weight (g) | Measurement Velocity (m/sec) | Shooting Distance (m) (calculated) |
|---|---|---|---|
| 990 | 1.7 (STD) | 990 | 0.0 |
| 933 | 1.6 | 930 | 50 |
| 885 | 1.5 | 865 | 100 |
| 790 | 1.4 | 810 | 150 |
| 695 | 1.3 | 755 | 200 |
| 680 | 1.2 | 700 | 250 |
| 665 | 1.1 | 650 | 300 |
| 625 | 1.0 | 600 | 350 |
| 585 | 0.9 | 555 | 400 |
| 545 | 0.8 | 510 | 450 |

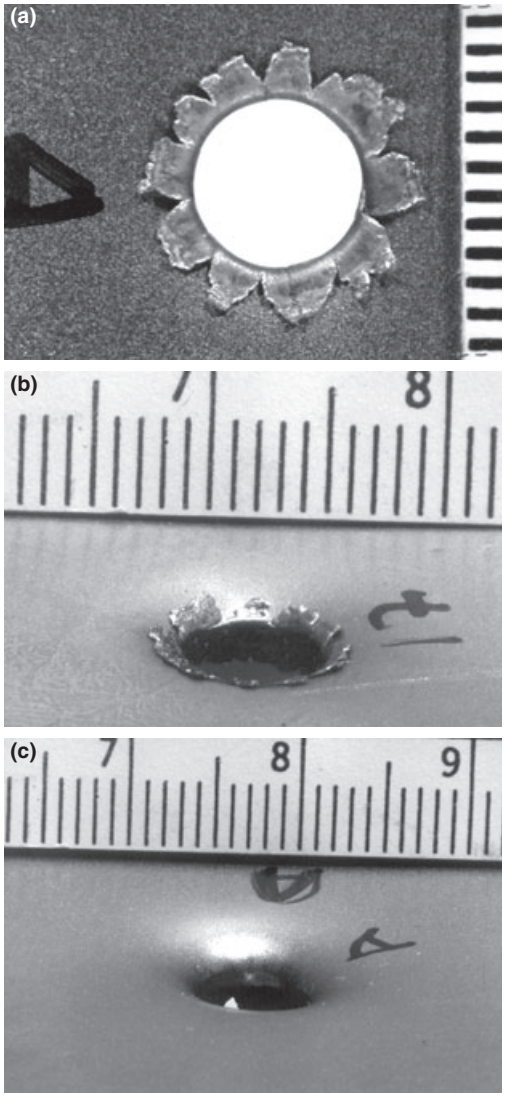


FIG. 1—*(a) High velocity petalling was created with no deformation contour on the metal plate. (b) Velocity 750 m/sec, petalling was not complete, and hole curvature had the shape of a funnel. (c) Velocity lower than 425 m/sec yielded pseudo-ellipsoid-shaped holes.*

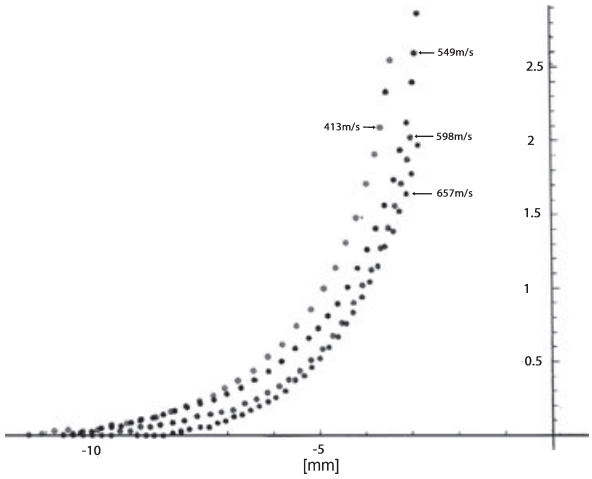


FIG. 2—*One side of shooting holes' shape in four velocities that hit the target.*

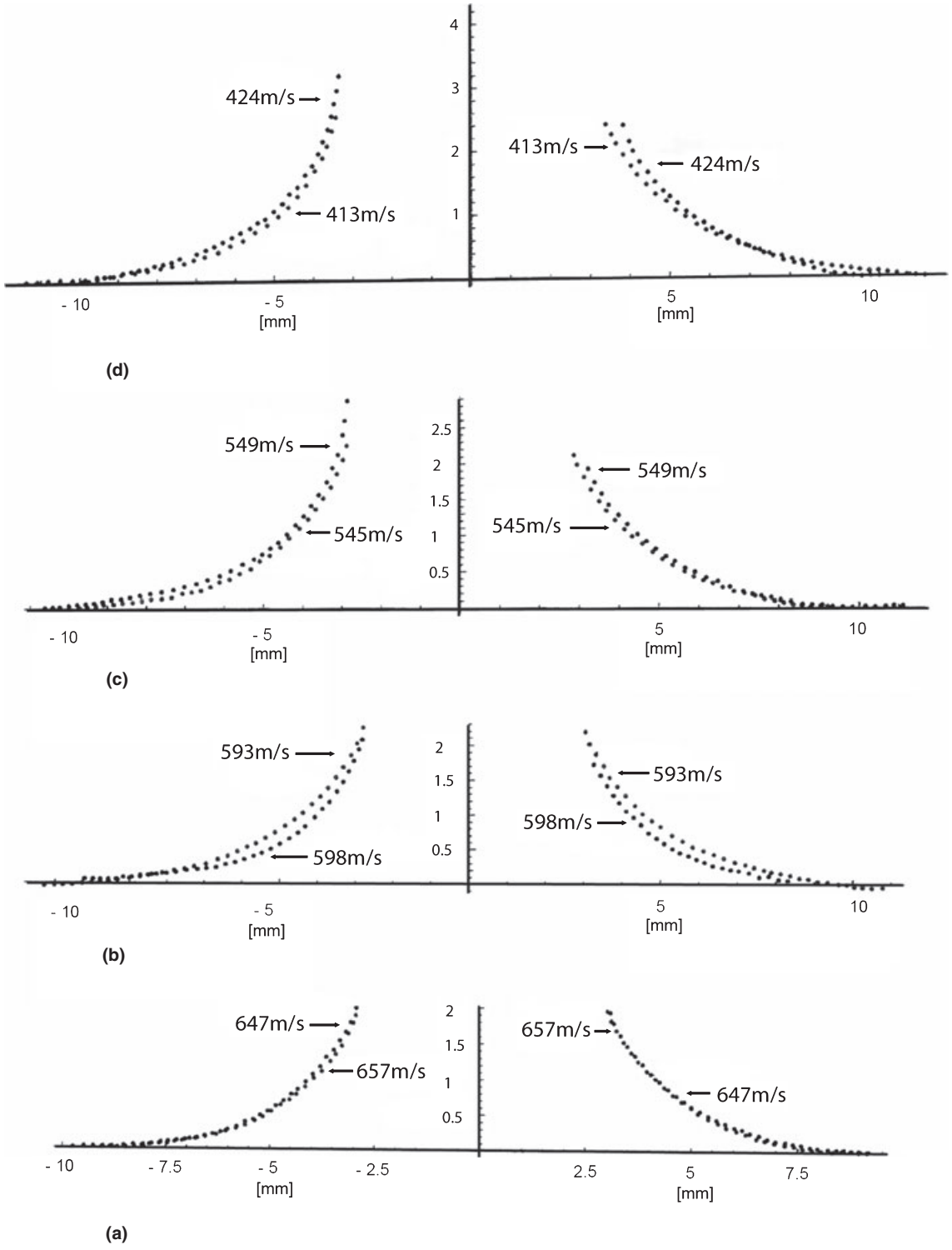


FIG. 3—*Repeatability of two extreme hole shapes in each shooting velocity in the 420–660 m/sec range. In high velocity (3d) the hole symmetry is better than in the low velocity (3a).*

## Results and Discussion

All the parameters that influence the behavior of the projectile during its flight were kept constant, including striking angle. The only parameter changed during the experiments was the projectile velocity.

Figures 1*a*–1*c* show the topographic shape of the holes created by the penetration of the projectiles into the metal targets at different velocities. High velocity petalling was created with no deformation contour on the metal plate. Petalling was not complete and the hole (curvature) had the shape of a funnel (Fig. 1*b*) at velocities lower than 750 m/sec. The funnel phenomenon increases as the velocity decreases. At velocities lower than 425 m/sec, the holes had a pseudo-elliptical shape (Fig. 1*c*).

Figure 2 illustrates the slope variation on one side of each penetrating hole. Each curve represents the variation of the distance

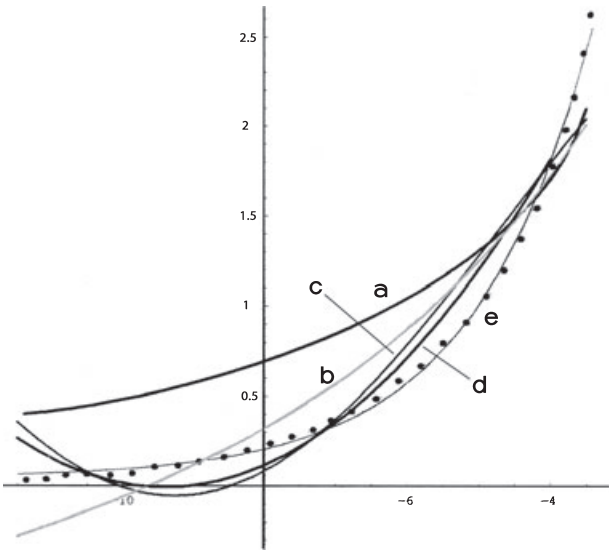


FIG. 4—*The chosen functions and their fit to the hole shape:*
*(a) cycloid* $Y = C - B\{\sqrt{2A * (E+x)^2} + A\arccos[1-(E+x)/A]\}$
*(b) Hyperbolic* $Y = A + \frac{B}{C+X}$
(*c*) Cosines $Y = a\cos bx$
(*d*) Parabolic $Y = A + BX^2$
(*e*) Exponential $Y_x = A + Be^{kx}$.

versus projectile velocity. The difference between the curvature and dimension of the holes is seen clearly. The curve slopes do not show linear behavior.

Two series of points were drawn on the graph for each velocity (between 420 and 660 m/sec). The series points were selected from the minimal and maximal contour-shaped holes from the same projectile velocity based upon experiment results (Fig. 3).

At high velocities (Fig. 3*d*), the hole symmetry is better than at low velocities (Fig. 3*a*). The relative asymmetry of the hole at the low velocities occurs due to the instability of projectile movement, therefore the two "contour sides" of the hole can be described by two different functions.

A function with physical meaning (not a polynomial from the "N" degree) and no linear behavior was searched (19) to obtain good fit to the curves (Fig. 4). The functions that were chosen are:

$$\text{Cycloid}: y = C - B\{\sqrt{2A^*(E+x)^2} + A\arccos[1-(E+x)/A]\}$$
$$\text{Hyperbolic}: Y = A + \frac{B}{C+X}$$

$$\text{Cosines}: Y = a\cos bx$$
$$\text{Parabolic}: Y = A + BX^2$$
$$\text{Exponential}: Y_x = A + Be^{kx}$$

Figure 4 shows the graphic behavior of all the detected functions to one of the hole contour. From this graph, it seems that the exponential function that best fits the curve is:

$$Y_x = A + Be^{kx} \tag{3}$$

where $A$ is asymptote of the function. For greater values of $X$ (in this case more then x > 10 mm), there is no deformation on the plate. $k$ is the curvature coefficient that describes the change of crumpling of the target. It is calculated from the two sides of the hole and describes the change rate of contour lines. The change is a function of the distances from the center of the hole. Function change will be greater when $k$ is bigger (in absolute value). "$B$" is the coefficient (there are two coefficients: $k$ and $B$) that describes the movement from the Y-axis. In this case, it describes the deepness of the spill. This behavior is dependant on the metal target property.

The greater be the coefficient $B$, the greater is the plastic deformation (crumpling). This happens due to the lower speed of the bullet. The $B$ value increases as the velocity decreases. This phenomenon is more pronounced for lower velocities.

The coordinates of the two sides of the holes were measured for each velocity. This provided two functions with two different $B$ coefficients. These different $B$ coefficients provide an asymmetrically shaped hole (Fig. 5). To eliminate this problem the researchers assumed "approximate symmetric axis" that determines an integrate one value of "B" representing the symmetric hole. This $B$ value is calculated from the meeting point of the two functions on the $Y$-axis. This point is perpendicular to the target from the two sides of the hole.

Figure 6 describes four groups of shooting distances and their fit regression function versus the hole's shape. Figure 6*a* is an overview of all the holes. Figure 6*b* is a magnification of the intersection virtual point when $X = 0$ (for every $B$).

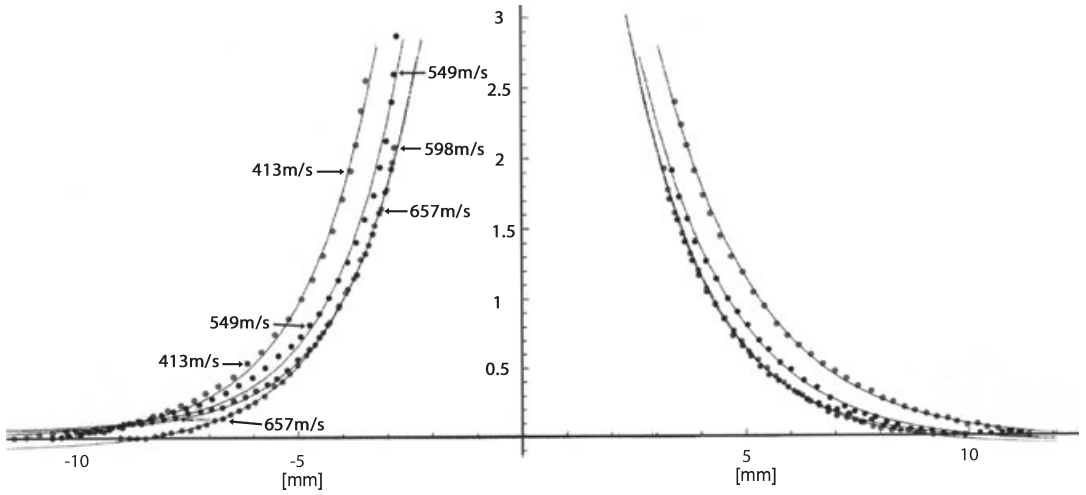


FIG. 5—*The two sides of the hole of four velocities. From these curves the* B *coefficient was calculated assuming "approximate symmetric axis."*

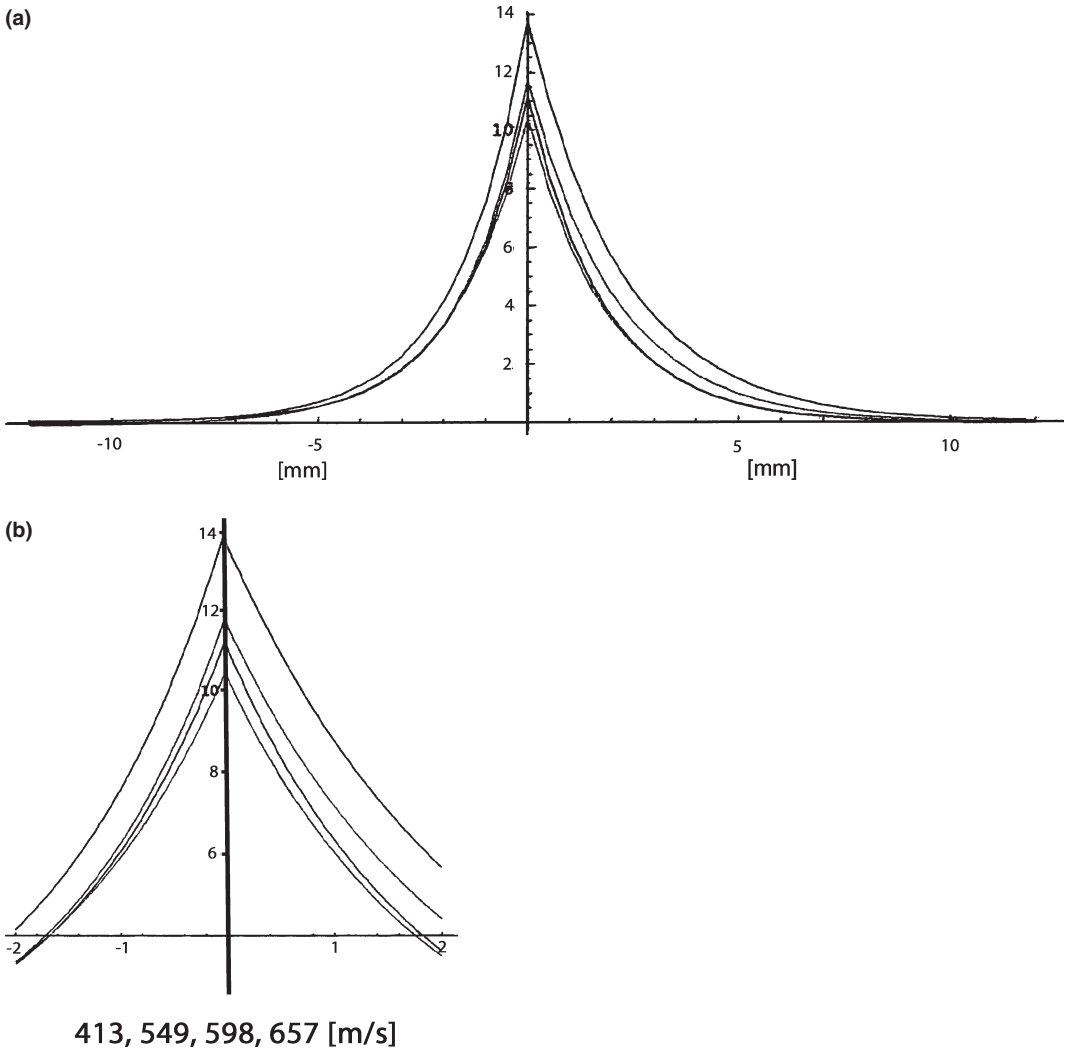


FIG. 6—*Finding the* B *coefficient of the exponential function, considering the two sides of the same hole. (a) Overview of all the holes. (b) Magnification of the intersection virtual point when* X = *0 (for every* B).

Table 2 shows the calculated values of $B$ and $k$ coefficients for each projectile velocity that reached the target.

To find the general equation of shooting distance, one takes the coordinates of the contour points from several known velocities. This equation describes the shooting distance versus velocity range between 400 and 700 m/sec according to shooting hole shapes. It is obvious that this equation needs to include velocity as one of the parameters as a result difference for different velocities. This parameter is entered in the equation in the denominator and the exponential. To fine-tune the equation, researchers increased the degree of freedom level by including power (mathematics exponent) to the velocity coefficient ($\alpha$), and to the exponential coefficient $1/\beta$ to the velocity. The equation shows

TABLE 2—*Calculated* B *and* k *coefficient values of both sides of the shooting hole for each projectile velocity while it reaches the target.*

| Coefficient $k_{(R)}$ | Coefficient $k_{(L)}$ | Coefficient $B$ | Velocity $V$ (m/sec) |
|---|---|---|---|
| −0.444 | 0.602 | 13.77 | 413 |
| −0.489 | 0.635 | 11.73 | 549 |
| −0.56 | 0.62 | 11.16 | 598 |
| −0.55 | 0.56 | 10.5 | 657 |

$$Y_{x,V} = \frac{B}{V^{\alpha}} e^{\left[\frac{k_X}{V^{\beta}}\right]} \tag{4}$$

The empirical solution of this equation based on the regression of shape coordinate hole of four velocities (413–657 m/sec) with $B$ parameter for each curve as described above is

$$Y_{x,V} = \frac{8.268}{V^{0.578018}} e^{\left(\frac{0.584x}{V^{0.005}}\right)} \tag{5}$$

Two sets of lines are described in Fig. 7: one set of lines corresponds to the experimental data from four different velocities found by Equation (3). The second line set corresponds to theoretical lines based on the regression that describes the line based in Equation (5).

The contour holes accuracy is better when using a small $x$ value (Fig. 7) on the chosen discriminate velocity, due to the difference between the lines. It becomes worse when a larger $x$ is used, due to the fact that all the lines are asymptotic and have a zero value on the $X$ axis. It is very important to define the zero point on the silicon cast on the axis (the place with no change) before ascertaining the coordinate's points from the silicon cast. With a small $x$ value, the range of mismatch between the graphs of the chosen

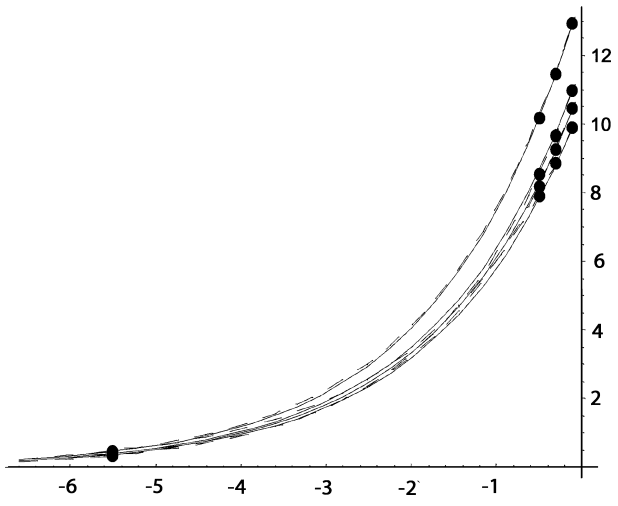


FIG. 7—*Describes two sets of lines: (a) One set of lines (full line) corresponds to its experimental line from four different velocities as they were calculated by Equation (3). (b) The second line set (dashed line) corresponds to theoretical lines based on the regression that describes the line based on Equation (5).*

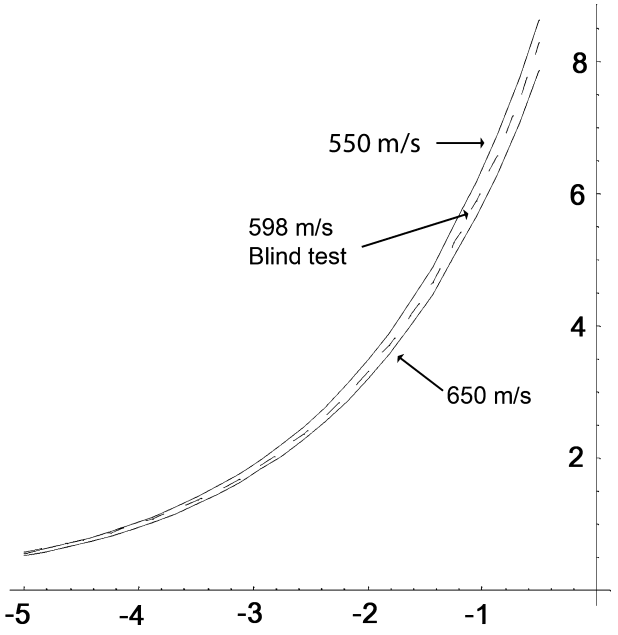


FIG. 8—*Blind test. Two extreme lines defined the velocities of 550–650 m/sec. The middle line is the "Blind Test" calculated by Equation (5).*

velocity and the empirical solution based on regression of the Equation (5) is smaller than the range between the chosen velocity lines.

A "blind test" was conducted on sets of coordinates that was measured along the hole contour (Fig. 8). The original axis was found by visual inspection, i.e., the place with no change along the *X* axis. The velocity found by empirical function (Equation 5) was 598 m/sec. (dashed line). Two regression lines that illustrate the velocity (Equation 3) are drawn in Fig. 8, one down and the other above the "blind test" line.

The "blind test" results show good fit to the result above when the holes are symmetric. One can clearly see the difference between the velocity lines in steps of 50 m/sec.

## Conclusion

This research presents an objective procedure for the estimation of the projectile velocity hitting the target, based upon the contours of entrance holes. The difference between the curvatures of the holes due to the velocity seems clear. The curve slope shows no linear behavior, and the best-fit function for all the holes is the exponential function.

The authors also found one function that describes the projectile velocity when it hits the target.

From Equation (5), the unknown velocity can be calculated by measuring the shape of the hole by finding the $k$ and $B$ coefficients from Equation (3). The reverse is also possible—finding the hole contour by knowing the velocity from Equation (5).

*Acknowledgments*

The authors would like to thank Mr. B. Glattstein and Mr. L. Nadivi for their assistance in the casework and collection of information and Prof. J. Levinson and E. Springer for their editorial assistance.

## References

1. Averbuch J. Mechanism approach to projectile penetration. J Technion Inst Technol 1970;8:375–83.
2. Averbuch J. Experimental and analytical investigation of the mechanism of projectile perforation in metallic plates (Ph.D thesis). Israel: Technion Institute of Technology, Material Engineering Department, 1970.
3. Warlow T. Firearms, the law and forensic ballistics, 2nd ed. Boca Raton, FL: CRC Press, 2005.
4. Kirk PL. Crime investigation, 2nd ed. New York: John Willey & Sons, 1974.
5. Alon D, Brando DG, Rosen A. An introduction to martial engineering. Haifa, Israel: Miclol (Technion), 1974 (in Hebrew).
6. Courtney M. Measuring bullet velocity with PC soundcard. Arxiv preprint physics/0601102, 2006, http://arxiv.org. Accessed November 6, 2008.
7. Saferstein R. Criminalistics: an introduction to forensic science. Upper Saddle River, NJ: Pearson Prentice Hall, 2007.
8. Glattstein B, Vinokurov A, Levin N, Zeichner A. Improved method for shooting distance estimation. Part 1: bullet holes in clothing items. J Forensic Sci 2000;45(4):801–6.
9. Ravreby M. Determination of firing distance by total nitrate. Proceedings of IDENTA 85, The International Congress on Techniques for Criminal Identification, 24–28 Feb, Jerusalem, Israel. Jerusalem, Israel: Heiliger and Co. Ltd., 1985;320–7.
10. Sellier K. Forensic science progress: shot range determination. Berlin: Springer-Verlag, 1991.
11. Nag NK, Sinha P. A note on assessability of firing distance from gunshot residues. Forensic Sci Int 1992;56:1–17.
12. Ravreby M. Analysis of long range bullet entrance holes by atomic absorption spectrophotometry and scanning electron microscopy. J Forensic Sci 1982;27(1):92–112.
13. Hagg LC. Bullet penetration and perforation of sheet metal. AFTE 1997;29(4):431–59.
14. Ben-Tovim U, Schecter B. Estimation of shooting distance from deformation bullet. AFTE 1993;25(1):31–8.
15. Nedivi L. Range estimation by use of simulation of bullet's deformation. Proceedings of the 35th Israel Annual Conference on Aerospace Science, Feb 15–16; Tel Aviv and Haifa, Israel. Haifa, Israel: Technion Institute of Technology, 1995;22–9.
16. Nennstiel R. Forensic aspects of bullet penetration of thin metal sheet. AFTE 1986;18(2):18–46.

17. Fackler M, Woychesin S, Dougherty P. Determination of shooting distance from deformation of the recovered bullet. J Forensic Sci 1987;32(4):1131–5.
18. Nennstiel R. Exterior ballistics computer software, EB Company, version 3.0, user's manual. Wiesbaden, Germany: EB Company, 1999.
19. Boas ML. Mathematical methods in the physical sciences. Hoboken, NJ: Wiley, 2006.

Additional information and reprint requests:
Tsadok Tsach, M.Sc.
Toolmarks and Materials Laboratory
DIFS, Israel Police Headquarters
Jerusalem 91906
Israel
E-mail: simanim@police.gov.il